

Sound Sensor Placement Strategy for Condition Monitoring of Induction Motor Bearing

Iradiratu Diah Prahmana Karyatanti^{1*}, Istiyo Winarno¹, Ardik Wijayanto², Dwisetiono³, Nuddin Harahab⁴, Ratno Bagus Edy Wibowo⁴ and Agus Budiarto⁴

¹Department of Electrical Engineering, Faculty of Engineering and Marine Science, Hang Tuah University, Jawa Timur 60111, Indonesia

²Department of Electronic Engineering, Electronic Engineering Polytechnic Institute of Surabaya, Jawa Timur 60111, Indonesia

³Department of Marine Engineering, Faculty of Engineering and Marine Science, Hang Tuah University, Jawa Timur 60111, Indonesia

⁴Environmental Science, Postgraduate, Brawijaya University, Malang, Jawa Timur 65145, Indonesia

ABSTRACT

Damage to the bearing elements will affect the rotation of the rotor and lead to the cessation of motor operation. Therefore, it is imperative to monitor the condition of the bearings to provide information on timely maintenance actions, improve reliability, and prevent serious damage. One of the important keys to an effective and accurate monitoring system is the placement of sensors and proper signal processing. Sound signal issued by the motor during operation capable of describing its elements' condition. Therefore, this study aims to develop a sound sensor placement strategy appropriate for monitoring the condition of induction motor bearing components. This study was carried out on three-phase induction motors' outer-race, inner-race, and ball-bearing sections with the signal processing method

using the spectrum analysis. Furthermore, the effect of sound sensor placement on condition monitoring accuracy was determined using the One-Way Analysis of Variance (One-Way ANOVA) approach. This process tests the null hypothesis and determines whether the average of all groups is the same (H₀) or different (H₁). Furthermore, Tukey's test was applied to obtain effective sound sensor placement, with voice-based condition monitoring used for effective identification. The test found

ARTICLE INFO

Article history:

Received: 26 November 2022

Accepted: 12 April 2023

Published: 09 October 2023

DOI: <https://doi.org/10.47836/pjst.31.6.25>

E-mail addresses:

iradiratu@hangtuah.ac.id (Iradiratu Diah Prahmana Karyatanti)

istiyo.winarno@hangtuah.ac.id (Istiyo Winarno)

ardik@pens.ac.id (Ardik Wijayanto)

dwisetiono@hangtuah.ac.id (Dwisetiono)

marmunnuddin@ub.ac.id (Nuddin Harahab)

rbagus@ub.ac.id (Ratno Bagus Edy Wibowo)

agusfpt@ub.ac.id (Agus Budiarto)

* Corresponding author

that the accuracy of monitoring the bearing condition was 92.66% by placing the sound sensor at 100 cm from the motor body.

Keywords: Bearing, condition monitoring, placement strategy, sound signal, spectrum analysis

INTRODUCTION

An induction motor is widely used as an industrial driving machine, while 90% serve as prime movers compared to other engine types (Gundewar & Kane, 2021). Damage to its parts can occur in the stator, rotor, bearings, and other parts. Bearing is one of the induction motor elements that play a significant role in aiding the rotating rotor. From the survey carried out by Toma et al. (2020), it was discovered that over 40% of the bearing gets damaged. It is caused by a lack of lubrication, inappropriate lubricants, incorrect installation, and overload. A monitoring system is needed to avoid its negative impact on motor parts. Furthermore, condition monitoring is necessary for industrial sustainability to boost efficiency, reliability, and safety, as well as reduce maintenance costs (Lee et al., 2021). The process was conducted by analyzing the sound generated by the motor during its operation. The advantage of this technique is that the microphone or sound sensor is relatively inexpensive, and its signal is easily captured without contact with the motor elements. This technique is usually recommended because it yields accurate results (Ewert et al., 2020).

The studies that discuss and monitor the condition of sound-based machine elements have been conducted using various signal-processing methods. Meanwhile, traditional signal processing techniques are still being developed by other research using time and frequency domain analyses, as well as a combination of both procedures (Chatterjee et al., 2020) because the adoption of Fast Fourier Transform (FFT) provides information about the condition of the motor elements. The signal in the time domain is transformed to the frequency analysis using the Fourier Series, Discrete Fourier Transform (DFT), and FFT. According to Nakamura et al. (2021), the advantage of frequency domain analysis is that it can identify signal components. Furthermore, to reduce the use of computer technology with high specifications, this technique is quite reliable and serves as an alternative system for monitoring the condition of induction motor elements (Qiao et al., 2020).

The placement of different sensor locations results in changes in sensitivity because they are affected by environmental noise around the induction motor. Zhang et al. (2020) stated that sensor placement greatly affects the accuracy of the monitoring diagnosis results. Furthermore, five sensors were placed at 30 cm to obtain detailed information concerning the bearing condition of a single-phase induction motor (Glowacz et al., 2018). Wang et al. (2019) adopted an efficient sensor placement strategy, using multi-sensors with a Multidimensional Time-Series Analysis approach. The result showed that the higher the

number of sensors used, the greater the information obtained, although this requires much money. For this reason, it is necessary to employ an effective strategy to ensure that the placement of the right sensor provides accurate monitoring information concerning the condition of the motor elements (Goyal et al., 2019). It is in addition to the proposals of a sensor placement strategy with a mathematical model based on the Response Surface Methodology (RSM) (Bhogal et al., 2015). RSM is a statistical model used to analyze problems in which several independent variables positively affect the response attribute. It led to the developing of a mathematical relationship model between input variables and response parameters to determine the optimal sensor placement for monitoring gearbox conditions with an accuracy of 92.2% (Vanraj et al., 2017).

Developing an efficient placement strategy is necessary to improve sensor data quality and monitoring accuracy. It enables the captured signal characteristics to represent the actual condition of the motor part. Therefore, this study discusses the strategy for placing sound sensors to monitor the condition of three-phase induction motor bearing elements. Spectrum analysis was employed in terms of executing this investigation. The independent variable is the microphone placement as a sound sensor subjected to six different distance treatments, with the mean difference evaluated using the ANOVA test. The results showed that environmental complexity affects the monitoring condition of the motor bearing as an industrial driving machine. Therefore, the sensor placement strategy is essential and contributes significantly to the industry.

MATERIALS AND METHODS

Generally, machine condition monitoring consists of three steps: collecting relevant data, processing and analyzing data, and diagnostic and prognostic decision-making (Goyal et al., 2021). An approach flowchart of the bearing condition monitoring, which focuses on sensor placement strategies, is shown in Figure 1. It captures the sound signal from the motor operation, and the placement is tested based on six varying distances measured from the motor body. The sound signal captured by the microphone is analog. Then, this signal will be converted to a digital signal by the Analog to Digital Converter (ADC). The resulting digital signal is still in the time domain, so a feature generation process step is needed to obtain a signal in the frequency domain (using the FFT algorithm). The bearing condition can be diagnosed using spectrum analysis. Spectrum analysis is a diagnostic approach employed to monitor the bearing conditions due to its frequency characteristics. The sound signal is processed with FFT to obtain a sign in the frequency domain. Meanwhile, the spectrum analysis is used to determine the condition of the outer and inner races, as well as the ball bearing in the induction motor rotor. Figure 2 shows the experimental setup of the bearing elements condition and monitoring system. The induction motor tested has specifications of 3 phases, 380 V, 3.68 A 1.5 kW, and 4 poles. Monitoring data is captured

using a sound sensor (USB microphone). The test bearing specifications are 6205 2R, with a bore diameter of 25 mm, an outer diameter of 52 mm, and a number of balls of 9 pieces. The motor load is in the form of a mechanical load. Therefore, artificial damage is carried out to prove the monitoring accuracy by providing defects in the outer race bearing, broken ball bearing, and healthy inner race. The developed monitoring system should recognize the conditions tested, as shown in Figure 3.

Spectrum analysis is a diagnostic approach employed to monitor the bearing conditions due to its frequency characteristics. The sound signal generated by a faulty motor operation conveys harmonic information. The flux density in the air gap becomes asymmetrical and affects the inductance, thereby increasing the amplitude at a certain frequency (Nirwan & Ramani, 2022). Meanwhile, the frequency of the bearing elements is determined from the geometry, kinematics, and rotational speed, where r , V , ω , N , d , D_p , and θ denote distance, linear speed, angular speed, number of *ball bearings*, diameter ball bearing, diameter pitch, and contact angle, respectively (Figure 4).

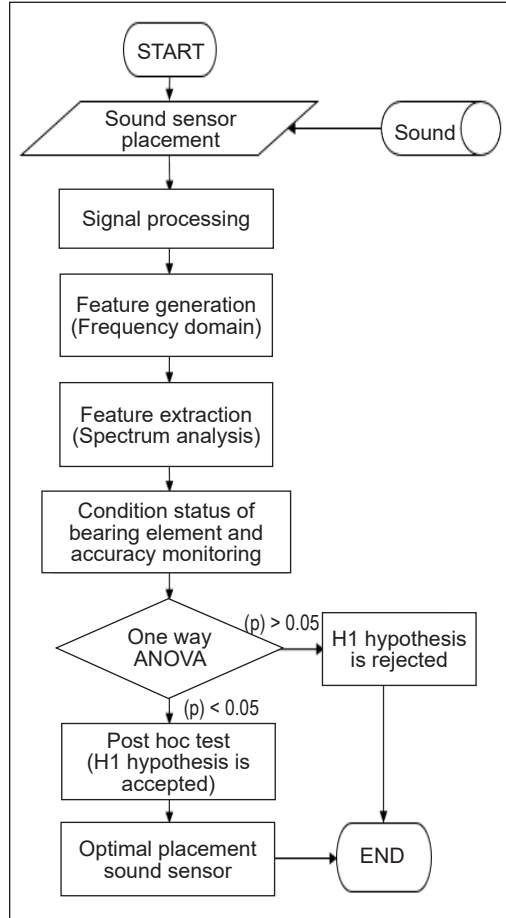


Figure 1. Flowchart of the proposed approach

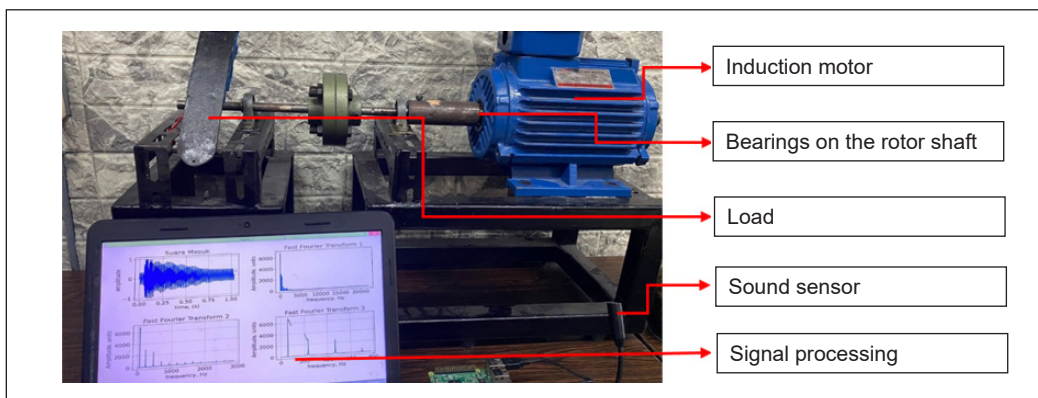


Figure 2. Experimental setup for monitoring condition-bearing

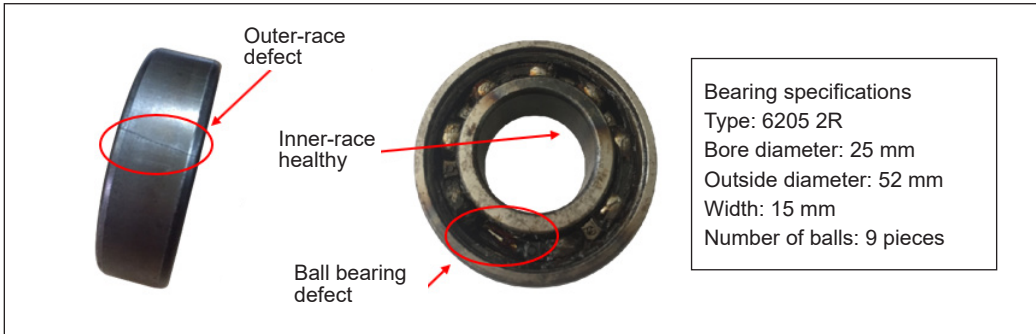


Figure 3. Bearing shaft rotor used for condition monitoring system test

When the bearing rotates, it produces a linear speed within the following range, as described in Equation 1:

$$V_c = \frac{V_i + V_o}{2} = \frac{\omega_i r_i + \omega_o r_o}{2} \quad (1)$$

where,

$$r_i = \frac{D_p}{2} - \frac{d \cos \theta}{2} \text{ and } r_o = \frac{D_p}{2} + \frac{d \cos \theta}{2}$$

$$V_c = \omega_c r_c = \omega_c \left(\frac{D_p}{2} \right) \text{ if } r_c = \frac{D_p}{2}$$

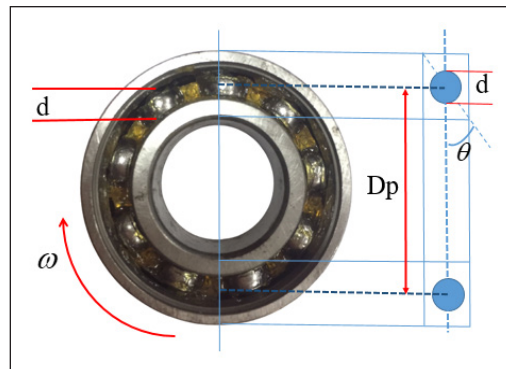


Figure 4. Bearing front view

Therefore, the angular speed of cage bearing formulated in Equation 2:

$$\omega_c = \left(\frac{2V_c}{D_p} \right) = \left(\frac{2}{D_p} \right) \cdot V_c = \left(\frac{2}{D_p} \right) \times \left(\frac{\omega_i r_i + \omega_o r_o}{2} \right) = \frac{\omega_i r_i + \omega_o r_o}{D_p} \quad (2)$$

The distance between the inner and outer races is as follows:

$$r_i = \frac{D_p}{2} - \frac{d \cos \theta}{2} \text{ and } r_o = \frac{D_p}{2} + \frac{d \cos \theta}{2}$$

Hence, the angular speed of the cage bearing is shown in Equation 3

$$\omega_c = \frac{\omega_i \left(\frac{D_p}{2} - \frac{d \cos \theta}{2} \right) + \omega_o \left(\frac{D_p}{2} + \frac{d \cos \theta}{2} \right)}{D_p} = \frac{1}{2} \left[\omega_i \left(1 - \frac{d \cos \theta}{D_p} \right) + \omega_o \left(1 + \frac{d \cos \theta}{D_p} \right) \right] \quad (3)$$

Because ω is $2\pi f$ then the frequency of cage bearing formulated in Equation 4:

$$f_c = \frac{1}{2} \left[f_i \left(1 - \frac{d \cos \theta}{D_p} \right) + f_o \left(1 + \frac{d \cos \theta}{D_p} \right) \right] \quad (4)$$

Additionally, a defect in the outer race causes a spike in amplitude at a certain frequency. Its bearing rotation frequency, namely the Ball Pass Frequency of Outer Race (BPFO), is calculated as follows:

$$f_{BPFO} = N(\omega_c - \omega_o) = \frac{N}{2}(f_i - f_o) \cdot \left(1 - \frac{d \cos \theta}{D_p}\right)$$

The outer race bearing frequency is assumed to be 0 because it is locked with the external casing, where the inner race and the motor rotor shaft frequency ($f_i = f_s$) are the same (Barusu & Deivasigamani, 2020). Therefore, the outer race bearing frequency formulated in Equation 5:

$$f_{BPFO} = \frac{N}{2} f_s \left(1 - \frac{d \cos \theta}{D_p}\right) \quad (5)$$

Similarly, the Ball Pass Frequency of Inner Race (BPFi) is shown in Equation 6:

$$f_{BPFi} = N(\omega_i - \omega_c) = \frac{N}{2}(f_i - f_o) \left(1 + \frac{d \cos \theta}{D_p}\right)$$

$$f_{BPFi} = \frac{N}{2} f_s \left(1 + \frac{d \cos \theta}{D_p}\right) \quad (6)$$

The ball bearing frequency can be formulated as Ball Spin Frequency (BSF) using the following equation:

$$\omega_r = \frac{V_r}{r_r} = \frac{(\omega_i - \omega_c)r_i}{r_r} = \frac{(\omega_i - \left\{ \frac{1}{2} \left[\omega_i \left(1 - \frac{d \cos \theta}{D_p}\right) + \omega_i \left(1 + \frac{d \cos \theta}{D_p}\right) \right] \right\})r_i}{r_r}$$

$$\omega_r = \frac{D_p}{2d} (\omega_i - \omega_o) \left[1 - \left(\frac{d \cos \theta}{D_p} \right)^2 \right] \text{ then } f_r = \frac{D_p}{2d} (f_i - f_o) \left[1 - \left(\frac{d \cos \theta}{D_p} \right)^2 \right]$$

The Ball Spin Frequency (BSF) is described in Equation 7:

$$f_{BSF} = f_r = \frac{D_p}{2d} f_s \left[1 - \left(\frac{d \cos \theta}{D_p} \right)^2 \right] \quad (7)$$

The characteristics of the sound signal at the f_{BPFO} , f_{BPFi} , and f_{BSF} frequencies indicate the condition of each bearing section.

Monitoring accuracy is proven by the percentage of correctness based on the condition of the bearing elements tested. Interestingly, a one-way ANOVA approach was used to test the hypothesis. This comparative evaluation examines the difference in the mean data of two or more groups. The hypothesis (H1) states that the sound sensor placement significantly affects the accuracy of monitoring the motor bearing condition. On the other hand, the (H0) hypothesis states that sensor placement has an insignificant effect on monitoring accuracy. The one-way ANOVA hypothesis test formulation is shown in Equation 8:

$$\begin{aligned}
 H_0 : \alpha_1 = \alpha_2 = \dots = \alpha_k \\
 H_1 = \text{not all group means are equal}
 \end{aligned}
 \tag{8}$$

Where α_k is the average group k , and k is the total number of groups. Assuming the one-way ANOVA test value states that (H_1) is accepted, a post hoc test is carried out to determine the optimal sensor placement. The approach proposed by Tukey (honestly significant difference) is a post hoc test that is applied if (H_0) is rejected (Shabbir et al., 2020). The Tukey test formula is shown in Equation 9:

$$|t| = \frac{|y_i - y_j|}{\sqrt{MSE \left(\frac{1}{n_i} + \frac{1}{n_j} \right)}} > \frac{1}{\sqrt{2}} q_{\alpha, k, N-k}
 \tag{9}$$

where the sample means of the group i and j are symbolized by y_i and y_j , MSE is a mean squared error, n_i and n_j are sample size group, $q_{\alpha, k, N-k}$ is Tukey table, α is the significance level, N is the total number of observations, and k is the number of groups.

RESULTS AND DISCUSSION

The microphone captures a signal in the time domain as a sound sensor. Sound data is retrieved for 30 seconds with a sampling frequency of 44.1 kHz. The data acquired in the time domain is transformed into that of the frequency using the FFT algorithm. Then, spectrum analysis is carried out by calculating the frequency of its characteristics to determine the condition of the bearing elements. Referring to the specifications in Figure 3 and the application of Equations 5, 6, and 7, the frequency of each bearing element is:

$$\begin{aligned}
 f_{BPFO} &= \frac{9}{2} 24.96 \left(1 - \frac{7.25 \cos 0^\circ}{38.5} \right) = 91.18 \text{ Hz} \\
 f_{BPFI} &= \frac{9}{2} 24.96 \left(1 + \frac{7.25 \cos 0^\circ}{38.5} \right) = 133.50 \text{ Hz} \\
 f_{BSF} &= \frac{38.5}{2 \times 7.25} 24.96 \left[1 - \left(\frac{7.25 \cos 0^\circ}{38.5} \right)^2 \right] = 43.67 \text{ Hz}
 \end{aligned}$$

The following 91.18 Hz, 133.50 Hz, and 43.67 Hz are the fundamental frequencies of the outer and inner races, as well as the ball bearing. Each frequency of the harmonic element bearing was further observed. A sample spectrum of 800 Hz generates 6, 8, and 18 frequencies at f_{BSF} , f_{BPFO} and f_{BPFI} . Therefore, one sample data spectrum analysis is used to observe the amplitude at 32 harmonic frequencies.

Figure 5 shows spectrum analysis at the fundamental frequency, where (a) depicts the sound spectrum with sensor placements of 50 cm, (b) 100 cm, and (c) 150 cm. The blue signal is the reference sound spectrum obtained from the operational bearing under a healthy condition, while the red is the test spectrum. If the test amplitude exceeds the

reference, the element bearing is declared to be in a damaged condition. On the other hand, assuming the reverse was the case, the element bearing is declared fit. Based on the test on the sensor placement of 50 cm from the motor body, the ball bearing was detected under a healthy condition; likewise, the outer race, while the inner one, was damaged. The monitoring results are inappropriate because the bearing elements were detected under damage conditions. In this case, the condition monitoring system is less accurate. However, this is different when reviewing the spectrum analysis results with the 100 cm sensor placement, as shown in Figure 5(b). The frequency of all bearing elements indicates the actual condition monitoring where the ball bearing and outer race are detected under faulty conditions while the inner one is in a healthy state. Figure 5(c) shows the sound spectrum with 150 cm sensor placement; the results of condition monitoring are less accurate.

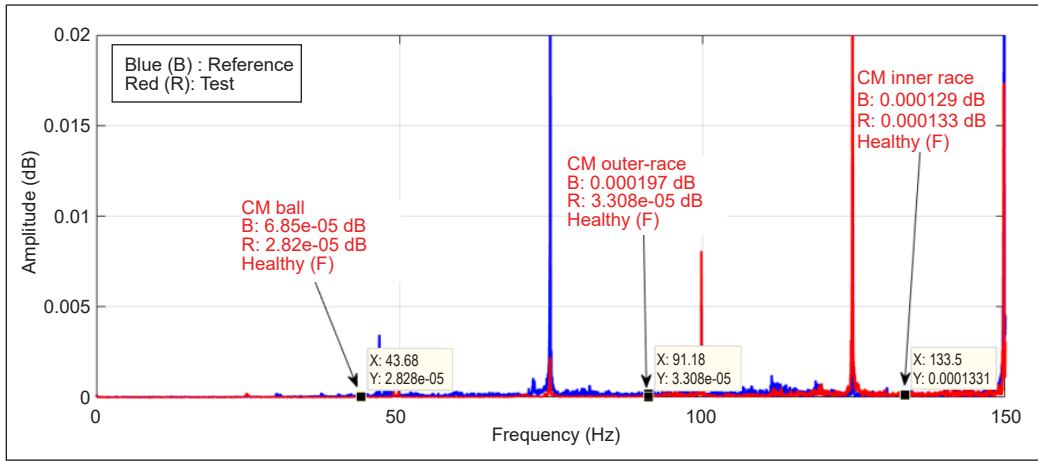
The condition monitoring results of the bearing elements up to the fourth harmonic frequency shown in Table 1 is a detailed test of the first data where accuracy is calculated based on the percentage truth for the condition monitoring results of all bearing elements. Data was retrieved on each sensor placement variation four times to get valid results.

The accuracy of the condition monitoring for all data repetitions is shown in Table 2. One-way ANOVA is performed using the data in Table 2 with respect to the hypothesis test. The requirements are that the sample data used should be normally distributed, its population must have a homogeneous variance, and the samples do not need to be related to each other. The normality test shows that the acquired information has been normally distributed with a P-value greater than 0.05, relatively 0.546. Meanwhile, the data homogeneity test was used to obtain a value of 0.275, meaning it is homogeneous.

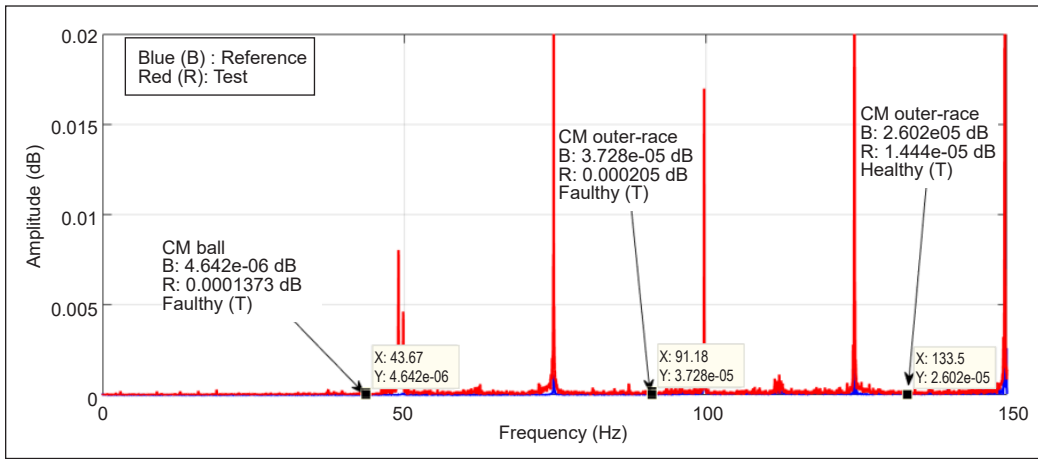
Table 3 is a one-way sensor placement ANOVA regarding accurately monitoring the bearing elements' conditions. It shows that the P-value is less than 5%. Therefore, it was concluded that (H1) is accepted, indicating that the sensor placement significantly affects the monitoring accuracy of bearing elements. The post hoc and Tukey tests were conducted to detect the best placement. Figure 6 shows the Tukey test results with a 95% confidence level. Based on the data grouping, the 100 cm sensor placement is the best location for monitoring the condition of bearing elements, with an average accuracy of 92.66%. Relatively high accuracy is achieved with the proposed approach, thereby being highly recommended as an alternative for monitoring the condition of an induction motor.

Similar studies are shown in Table 4 as a discourse on developing motor condition monitoring. It also depicts studies that discuss monitoring the condition of motor elements based on sound and vibration data, where both are strongly influenced by ambient noise. Previous analyses presented this challenge to develop a condition-monitoring system by examining the effect of noise on accuracy (AlShorman et al., 2021). Therefore, the present study examines the optimal and effective sensor placement because the sound is susceptible to ambient noise.

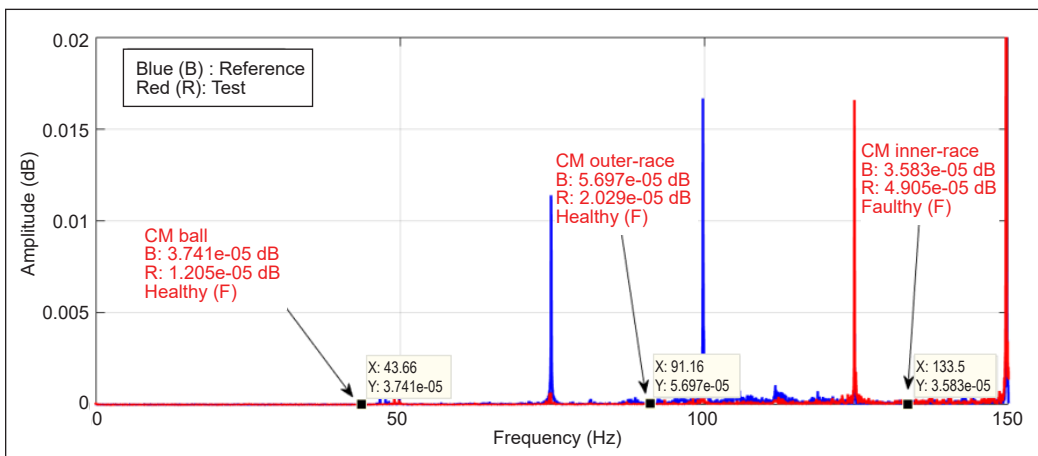
Sound Sensor Placement Strategy



(a)



(b)



(c)

Figure 5. Spectrum analysis on the different sensor placements: (a) 50 cm; (b) 100 cm; and (c) 150 cm

Table 1
Spectrum analysis for condition monitoring and detection accuracy

Placement	Bearing Condition	Freq (Hz)	Amplitude (dB)		Result	Accuracy (%)
			Ref	Test		
50 cm	Ball bearing defect	f	0.000068	0.000028	False	49.07 %
		f_{x2}	0.000121	0.000038	False	
		f_{x3}	0.000168	0.000071	False	
		f_{x4}	0.003058	0.004393	True	
	Outer-race defect	f	0.000197	0.000033	False	
		f_{x2}	0.000190	0.000218	True	
		f_{x3}	0.000174	0.000237	True	
		f_{x4}	0.000138	0.000203	True	
	Inner-race healthy	f	0.000129	0.000133	False	
		f_{x2}	0.000158	0.000227	False	
		f_{x3}	0.000387	0.000633	False	
		f_{x4}	0.000157	0.000359	False	
100 cm	Ball bearing defect	f	0.000004	0.000137	True	94.44 %
		f_{x2}	0.000018	0.000288	True	
		f_{x3}	0.000032	0.000109	True	
		f_{x4}	0.006436	0.056430	True	
	Outer-race defect	f	0.000037	0.000205	True	
		f_{x2}	0.000138	0.000425	True	
		f_{x3}	0.000018	0.000279	True	
		f_{x4}	0.000191	0.000199	True	
	Inner-race healthy	f	0.000026	0.000014	True	
		f_{x2}	0.000138	0.000077	True	
		f_{x3}	0.000310	0.000242	True	
		f_{x4}	0.000228	0.000139	True	
150 cm	Ball bearing defect	f	0.000037	0.000012	False	60.55 %
		f_{x2}	0.000037	0.000073	True	
		f_{x3}	0.000055	0.000067	True	
		f_{x4}	0.008330	0.035380	True	
	Outer-race defect	f	0.000056	0.000020	False	
		f_{x2}	0.000079	0.000171	True	
		f_{x3}	0.000168	0.000506	True	
		f_{x4}	0.000204	0.000216	True	
	Inner-race healthy	f	0.000035	0.000049	False	
		f_{x2}	0.000351	0.000106	True	
		f_{x3}	0.000107	0.000077	True	
		f_{x4}	0.000298	0.000620	False	

Table 2
Detection accuracy in all test cases

Placement (cm)	Repetition (r)				Average
	1	2	3	4	
0	13,33 %	15,18 %	20 %	24,16 %	18,17 %
50	49,07 %	60,55 %	47,87 %	56,38 %	53,47 %
100	94,44 %	87,77 %	92,12 %	96,29 %	92,66 %
150	60,55 %	56,20 %	58,70 %	54,53 %	57,49 %
200	59,90 %	44,90 %	57,59 %	50,92 %	53,33 %
250	50,18 %	41,85 %	47,87 %	52,03 %	47,98 %

Table 3
One-way analysis of variance placement sensor

Source of Diversity	Degrees Free	Sum of squares	Middle square	F-Value	P-Value
Treatment	5	11308.4	2261.68	92.57	0.000
Galat	18	439.8	24.43		
Total	23	11748.2			

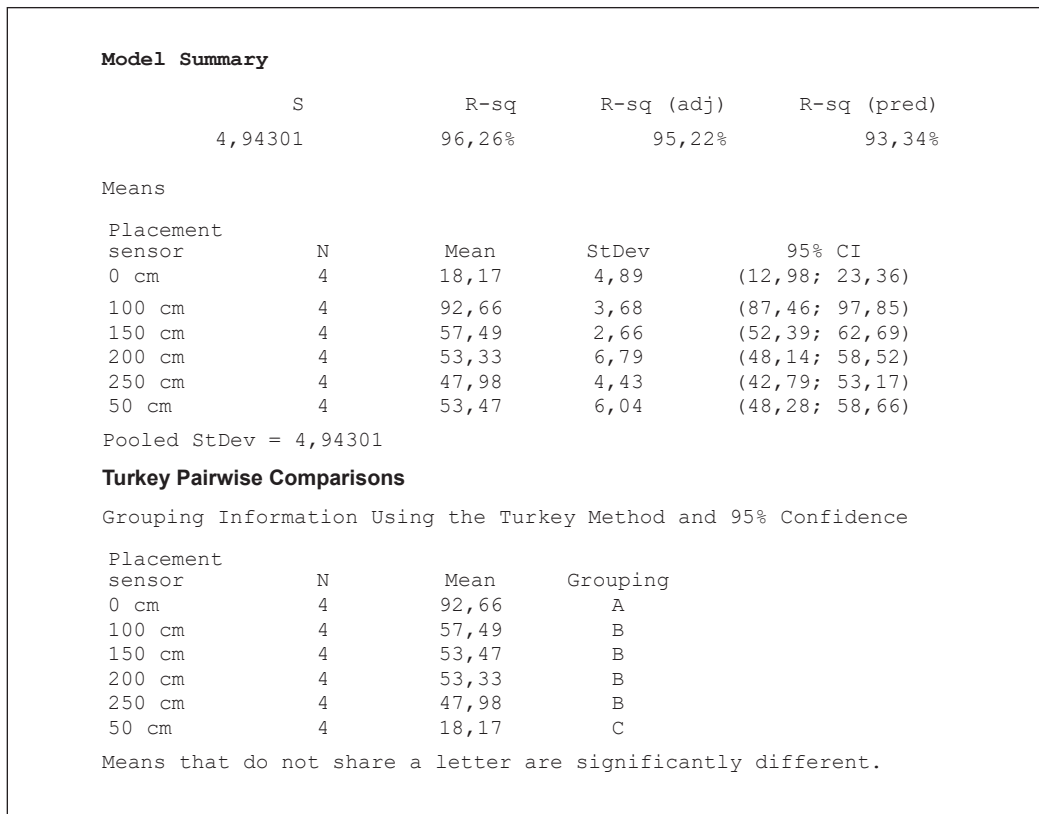


Figure 6. Tukey test

Table 4
Comparison of similar research with proposed research

Reference	Feature extraction method	Sensor	Placement strategy	Highlight
Vanraj et al., 2017	No discussion	Microphone	RSM	Sensor placement strategy using RSM approach with 112.5 cm.
Glowacs et al., 2018	MSAF-20-MULTIEXPANDED	Microphone	30 cm sensor placement	The sensor placement strategy approach is not discussed.
Wang et al., 2019	MultiDTSA and ARIMA	Microphone and accelerometer	No discussion	Future studies are recommended to optimize sensor settings.
Vamsi et al., 2019	wavelet decomposition	Microphone and accelerometer	No discussion	The placement of the sound sensor is free and more accurate than that of the vibration.
Goyal et al., 2019	FFT	Accelerometer	NC-OSP strategy	RSM can be used to track the optimal non-contact sensor location.
Nirwan & Ramani, 2022	FFT	Microphone, Accelerometer	No discussion	The bearing monitoring results using sound data are better than a vibration.
Zhang et al., 2020	FFT	Accelerometer	No discussion	A sound and vibration sensor placement strategy is needed to get high accuracy.
AlShorman et al., 2021	Review all technique	Microphone	No discussion	Review, challenges, and future trends are discussed for developing the effect of noise on monitoring accuracy. This factor may be affected by providing the sensor placement treatment.
Proposed method	Spectrum analysis	Microphone	One way ANOVA	The sensor placement is the best strategy to get the accuracy of bearing elements monitoring.

CONCLUSION

The sound characteristics are used to describe the condition of the motor elements, and their monitoring is strongly influenced by ambient noise. The right placement of the sound sensor is extremely important in determining the follow-up actions for motor maintenance. It provides an opportunity for the noise signal to overlap with that generated by the operation of the motor. Furthermore, spectrum analysis is a reliable solution for monitoring the condition of bearing elements with an overview of its conditions strongly influenced by sound sensor placement. The accuracy of bearing elements monitoring is determined using the One-way ANOVA test. Based on the Tukey test, the placement of the sensor 100 cm from the motor body gives the best accuracy of all treatments, which is 92.66%. Future studies are expected to examine the sensor placement in more

detail because the treatment applied in the present study has a difference of 50 cm. This research contributes to the right sensor placement strategy to obtain accurate monitoring results. It enables the industrial community to carry out diagnostics and prognostics of the motor as the main driver.

ACKNOWLEDGEMENTS

The authors are grateful to the Electrical Machinery Laboratory and Energy Conversion Laboratory research team at Hang Tuah University, Indonesia, for their many contributions to this study.

REFERENCES

- AlShorman, O., Alkhatni, F., Masadeh, M., Irfan, M., Glowacz, A., Althobiani, F., Kozik, J. & Glowacz, W. (2021). Sounds and acoustic emission-based early fault diagnosis of induction motor: A review study. *Advances in Mechanical Engineering*, 13(2), 1-19. <https://doi.org/10.1177/1687814021996915>
- Barusu, M. R., & Deivasigamani, M. (2020). Non-invasive vibration measurement for diagnosis of bearing faults in 3-phase squirrel cage induction motor using microwave sensor. *IEEE Sensors Journal*, 21(2), 1026-1039. <https://doi.org/10.1109/JSEN.2020.3004515>
- Bhogal, S. S., Sindhu, C., Dhama, S. S., & Pabla, B. S. (2015). Minimization of surface roughness and tool vibration in CNC milling operation. *Journal of Optimization*, 2015, Article 192030. <https://doi.org/10.1155/2015/192030>
- Chatterjee, S., Barman, R., Roy, S. & Dey, S. (2020, December 16-19). *Bearing fault detection in induction motors employing difference visibility graph*. [Paper presentation]. 2020 IEEE International Conference on Power Electronics, Drives and Energy Systems (PEDES), Rajasthan, India. <https://doi.org/10.1109/PEDES49360.2020.9379635>
- Ewert, P., Kowalski, C. T., & Orłowska-Kowalska, T. (2020). Low-cost monitoring and diagnosis system for rolling bearing faults of the induction motor based on neural network approach. *Electronics*, 9(9), Article 1334. <https://doi.org/10.3390/electronics9091334>
- Glowacz, A., Glowacz, W., Glowacz, Z., & Kozik, J. (2018). Early fault diagnosis of bearing and stator faults of the single-phase induction motor using acoustic signals. *Measurement*, 113, 1-9. <https://doi.org/10.1016/j.measurement.2017.08.036>
- Goyal, D., Mongia, C., & Sehgal, S. (2021). Applications of digital signal processing in monitoring machining processes and rotary components: A review. *IEEE Sensors Journal*, 21(7), 8780-8804. <https://doi.org/10.1109/JSEN.2021.3050718>
- Goyal, D., Pabla, B. S., & Dhama, S. S. (2019). Non-contact sensor placement strategy for condition monitoring of rotating machine-elements. *Engineering Science and Technology, an International Journal*, 22(2), 489-501. <https://doi.org/10.1016/j.jestch.2018.12.006>
- Gundewar, S. K., & Kane, P. V. (2021). Condition monitoring and fault diagnosis of induction motor. *Journal of Vibration Engineering & Technologies*, 9(4), 643-674. <https://doi.org/10.1007/s42417-020-00253-y>

- Lee, W. J., Xia, K., Denton, N. L., Ribeiro, B., & Sutherland, J. W. (2021). Development of a speed invariant deep learning model with application to condition monitoring of rotating machinery. *Journal of Intelligent Manufacturing*, *32*(2), 393-406. <https://doi.org/10.1007/s10845-020-01578-x>
- Nakamura, H., Asano, K., Usuda, S., & Mizuno, Y. (2021). A diagnosis method of bearing and stator fault in motor using rotating sound based on deep learning. *Energies*, *14*(5), Article 1319. <https://doi.org/10.3390/en14051319>
- Nirwan, N. W., & Ramani, H. B. (2022). Condition monitoring and fault detection in roller bearing used in rolling mill by acoustic emission and vibration analysis. *Proceedings of Materials Today*, *51*, 344-354. <https://doi.org/10.1016/j.matpr.2021.05.447>
- Qiao, M., Yan, S., Tang, X., & Xu, C. (2020). Deep convolutional and LSTM recurrent neural networks for rolling bearing fault diagnosis under strong noises and variable loads. *IEEE Access*, *8*, 66257-66269. <https://doi.org/doi:10.1109/access.2020.2985617>
- Shabbir, M. N. S. K., Liang, X., & Chakrabarti, S. (2020). An ANOVA-based fault diagnosis approach for variable frequency drive-fed induction motors. *IEEE Transactions on Energy Conversion*, *36*(1), 500-512. <https://doi.org/10.1109/TEC.2020.3003838>
- Toma, R. N., Prosvirin, A. E., & Kim, J. M. (2020). Bearing fault diagnosis of induction motors using a genetic algorithm and machine learning classifiers. *Sensors*, *20*(7), Article 1884. <https://doi.org/10.3390/s20071884>
- Vamsi, I., Sabareesh, G. R., & Penumakala, P. K. (2019). Comparison of condition monitoring techniques in assessing fault severity for a wind turbine gearbox under non-stationary loading. *Mechanical Systems and Signal Processing*, *124*, 1-20. <https://doi.org/10.1016/j.ymssp.2019.01.038>
- Vanraj, Dhami, S. S., & Pabla, B. S. (2017). Optimization of sound sensor placement for condition monitoring of fixed-axis gearbox. *Cogent Engineering*, *4*(1), Article 1345673. <https://doi.org/10.1080/23311916.2017.1345673>
- Wang, T., Lu, G., & Yan, P. (2019). Multi-sensors based condition monitoring of rotary machines: An approach of multidimensional time-series analysis. *Measurement*, *134*, 326-335. <https://doi.org/10.1016/j.measurement.2018.10.089>
- Zhang, S., Wang, B., Kanemaru, M., Lin, C., Liu, D., Miyoshi, M., Teo, K. H., & Habetler, T. G. (2020). Model-based analysis and quantification of bearing faults in induction machines. *IEEE Transactions on Industry Applications*, *56*(3), pp.2158-2170. <https://doi.org/10.1109/tia.2020.2979383>